Earthline Journal of Mathematical Sciences
E-ISSN: 2581-8147
Volume 15, Number 6, 2025, Pages 989-1020
https://doi.org/10.34198/ejms.15625.9891020

Stochastic Dynamics of Dual-Prey–Predator Interactions under Harvesting Pressure: Insights from the California Current Ecosystem

Chandrima Talapatra

Department of Mathematics, Techno Main Salt Lake, EM 4/1, Sector V, Salt Lake, Kolkata 700091, India

ORCID: https://orcid.org/0000-0002-0569-8749

e-mail: c.talapatra.tmsl@ticollege.org

Abstract

This study presents a stochastic predator-prey model involving two harvested prey species—sardines and anchovies—and a common predator, the blacktip shark, under the influence of environmental noise. The model incorporates Holling type-II functional responses, harvesting efforts, and white noise perturbations representing environmental variability. Analytical investigations determine the boundedness and stability conditions of equilibria. Numerical simulations reveal that the predator population is highly sensitive to stochastic perturbations, particularly the noise intensity associated with predator mortality. Notably, a sufficiently large noise intensity in anchovy dynamics ($\alpha_2 > 72.06$) can stabilize the coexistence equilibrium, where higher values of α_1 and α_2 tend to destabilize the system. Phase portraits and bifurcation analyses illustrate the effects of harvesting rates and noise intensities on species persistence and extinction. These findings highlight critical thresholds for sustainable harvesting and noise tolerance, offering ecological insights into species coexistence within the California Current ecosystem.

1 Introduction

The California Current Ecosystem (CCE) ranks among the world's most productive marine systems. It supports diverse marine animals and hosts large commercial fisheries. Forage fish such as sardines (Sardinops sagax) and anchovies (Engraulis mordax) make up the component parts of this ecosystem, with these two forage fish types being consumed by a variety of predatory fishes, including blacktip sharks (Carcharhinus limbatus), tunas, and mackerels. The populations are thought to fluctuate greatly due to some stochastic elements and overexploitation by people [1, 2].

Understanding the demographic differences between these species is critical for the advancement of an ecosystem-based approach to fisheries management. Much of the competition between the sardines and

Received: July 20, 2025; Accepted: August 29, 2025; Published: September 9, 2025
2020 Mathematics Subject Classification: Primary 92D25, 60H10; Secondary 37H10, 92D40, 37N25.
Keywords and phrases: Holling type-II response, harvesting pressure, stochastic dynamics, stability analysis, stochastic persistence, stationary distribution, predator–prey model, environmental noise.

the anchovies is often referred to as "apparent competition," meaning that the two species' relationships are mediated through predators rather than through direct resource competition [3]. Climate, predation intensity, and harvesting regulations all define these phenomena.

Like every other ecosystem, marine ecosystems too depend on multiple stochastic factors such as the sea surface temperature (SST), climatic oscillations like El Nino Southern Oscillation (ENSO), and even ocean upwelling [4]. Sea surface temperature changes greatly impact recruitment, cycles in population, and species dominance. A series of studies suggest that whereas cooler conditions tend to benefit anchovies, warmer conditions tend to favor capacity of sardine populations [5].

Stochasticity is announced as an umbrella term that defines the SDEs, which are often used in determining the fluctuations in populations and the risks of their extinction [6]. These models are helpful in forecasting population persistence and the conditions in which they may sustain themselves despite the changes in the environment.

The present study highlights the effect of environmental fluctuations on the aquatic ecosystem. A number of researchers have analyzed the local and global dynamics of various prey models in a deterministic environment, as mentioned in [7], [8], [9], [10]. The drawback of the deterministic models is that they fail to justify the influence of environmental fluctuations. On the other hand, the parameters of the aquatic environment are random by nature, for instance, growth rate, mortality rate, density of species, etc.

They depend upon changes in nutrient and mineral supplies, levels of sun energy, oxygen, carbon dioxide concentration, concentration of nitrogen at some level in the sea, water salinity, the rate of flow, availability of food supply, unexpected appearances of poisonous agents, the maturation behavior of the organism, influences exerted by climatic fluctuations as seasonal change over the area, and thousands of such elements. May [11] said that continuous fluctuations in the environment affect birth and death rates, carrying capacity, competition coefficients, and all other parameters of the model. It is impossible to achieve a constant value for the equilibrium population distribution, which fluctuates around an average value. Many authors considered the impacts of white noise on two species of predator-prey models with various kinds of functional responses, as well as with other different kinds of responses ([12], [13], [14], [15]).

Few articles about a stochastic model of a predator-prey system with a Holling type II functional response have been written. J. Lv et al. [16] considered the dynamic properties of the stochastic model, and it is also devoted to the global stability of the positive solutions and discussed the stochastic persistence in the mean of the species population. In accordance with this, Z. Liu et al. [17] solved the stochastic prey-predator model with Holling type II and discussed the existence of a stationary distribution for small white noise. They analyzed the extinction of the system for large values of white noise. P. S. Mandal et al. [18] also considered a two-dimensional Holling-Tanner-type predator-prey model with stochastic perturbation and established that the system is strongly persistent on average when the intensity of

the environmental pressure is less than certain thresholds. Gard [19] considered the transient effects of stochastic multi-population models and estimated the exit probability, indicating the initial tendency of the corresponding populations in the system to survive or die out.

There is no unique way to formulate a stochastic model for interacting populations under discussion. The relationship between fluctuations and species concentration is measured by quantifying these variations in the model, which concerns noisy quantities whose variance at a given time may be a significant fraction of their mean values. The birth and death processes are inherently stochastic processes that depend on the average level of biomass and can vary rapidly from time to time. Since the interactions between populations are not uniformly distributed, there are some random factors in the system. These factors can be included in the mathematical model by taking into account parameters that fluctuate irregularly and randomly in nature. However, to the best of our knowledge, the analysis of fishery systems in the presence of environmental factors has not been addressed so far. Stochastic models can be broadly classified into two categories: discrete or continuous Markov chain modeling ([20], [21], [22]) and the noisy systems ([23], [24], [25]).

Fokker-Planck equations and moment closure techniques are some of the mathematical methods designed to find stationary distributions in stochastic ecological models [26]. In the context of the CCE, these techniques aid in the prediction of sardine and anchovy population dynamics in relation to changing environmental and fishing activities [27]. In ecological modeling, a principal question of interest is whether a given species endures in the face of stochastic influences and harvesting. This can be approached by persistence measures, extinction probabilities, invariant measures, and stationary distributions [28]. The stationary distribution of a species' population informs what the long-term changes of the species are and the probability of its occurrence at certain levels of abundance. This study is particularly applicable for understanding long-term species behaviors of sardines and anchovies in the California Current Ecosystem, in which stochastic environmental factors play an important role in population fluctuations.

Stability analysis of harvested predator-prey systems often uses equilibrium points, Lyapunov functions, and bifurcation analysis [29]. Some of the more recent studies have looked into how harvesting policies can be crafted to maximize profits economically while being ecologically sustainable [30]. In particular, bioeconomic models that include randomization of harvesting rates have been created in order to determine sustainability over a long period [31]. Since the natural growth and death rate of species in the ecosystem is often subject to environmental noise, many authors have investigated stochastic population models with harvesting ([32], [33], [34]). Harvesting natural populations is beneficial for commercial purposes, and its consequences or aftereffects are useful for renewable resource management ([32]- [35]). Harvesting can also mean a reduction in the population through hunting or trapping of individuals, effectively removing individuals from the population [36]. The capture intensity of harvesting depends mainly on the harvesting strategy used. The capture function plays a key role in describing the dynamic behavior of the

predator-prey system.

An essential aspect of ecological modeling is establishing whether a species can survive in the long run while experiencing random effects along with harvesting. A person's capability to investigate persistence can be done through extinction probabilities, invariant measures, and stationary distributions [28]. It is always good to know the stationary distribution of the population of a species because it gives information on its future long-run fluctuations and the extent of abundance of the species.

In this paper, a stochastic predator–prey model involving two prey species and a common predator has been investigated. Intra-specific competition is assumed within the predator population, while interspecific competition occurs between the two prey species. Additionally, harvesting pressure is incorporated on the prey populations in the presence of environmental stochasticity.

The modeling framework and analysis proceed as follows: A comprehensive stochastic differential equation (SDE) model has been considered in Section 2 by introducing white noise into the intrinsic growth rates of the prey and the mortality rate of the predator, while all other parameters remain deterministic. Section 3 establishes the stochastic stability of the system in the mean-square sense near the interior equilibrium. Section 4 demonstrates the existence of a unique positive global solution to the stochastic model. Section 5 derives the parametric thresholds required to ensure stochastic persistence in the mean for all species. The long-term behavior of the system is explored in Section 6, where we investigate the existence of a stationary distribution under suitable conditions. The theoretical results are illustrated through numerical simulations in Section 7, validating the effects of environmental noise and harvesting on population dynamics. Finally, ecological interpretations of the findings and their implications for species persistence and management are discussed in Section 8.

2 Mathematical Model Formulation

A classic example of a system with two prey animals and one predator can be seen in the ecosystem of the California Current on the west coast of North America. In this marine ecosystem, sardines (Sardinops sagax) and anchovies (Engraulis mordax) are the prey. These two species are commercially harvested because of their high economic value, mainly for human consumption, aquaculture, and fish-meal production. These two small pelagic fish species are indirectly competing, also known as false competition, because they are important prey for these generalist predators, among others such as the blacktip shark (Carcharhinus limbatus) and large predatory fish such as tuna and mackerel.

Within this system, the predator population represented by the blacktip shark feeds upon both prey species to create some complex dynamics in predator-prey interactions. This fishery is within the California Current, where sardine and anchovy fisheries are closely monitored and mostly managed to

avoid overfishing, for fluctuations in prey could directly affect the predator population and eventually the stability of the ecosystem. Moreover, the predatory fish population in that region, the blacktip shark, is not fished since conservation efforts aim at averting the further decline of sharks.

This interplay between the continuous removal of prey and the feeding behavior of predators illustrates the complicated dynamics of this marine ecosystem, which is shaped by both natural ecological processes and human activities. Such a system can be mathematically modeled to understand the interactions between the two prey species (sardines and anchovies) and their common predator (the blacktip shark) and to gain insights into the sustainability and stability of the ecosystem under different fishing scenarios.

For simplicity, logistic growth functions are assumed for both sardines and anchovies, implying that the population density of each species is resource-limited. It is also assumed that the feeding rate of the predator (blacktip shark) increases linearly with prey density, while the functional response of the predator is described by a Holling type II functional response.

The governing equations of the system can be formulated as follows:

$$\begin{aligned} \frac{dx_1}{dt} &= x_1\left(a_1 - x_1 - \frac{c_1 y}{e_1 + x_1} - E_1\right), \\ \frac{dx_2}{dt} &= x_2\left(a_2 - x_2 - \frac{c_2 y}{e_2 + x_2} - E_2\right), \\ \frac{dy}{dt} &= y\left(\frac{m_1 x_1}{e_1 + x_1} + \frac{m_2 x_2}{e_2 + x_2} - d_1 - \gamma y\right), \end{aligned} \tag{1}$$

where:

- x_1 and x_2 denote the biomass of the prey species, sardines and anchovies, at time t.
- y denotes the biomass of the predator population (blacktip shark) at time t.
- a_1 and a_2 are the intrinsic birth rates of sardines and anchovies, respectively.
- c_1 and c_2 are the per capita predation rates of the blacktip shark on sardines and anchovies.
- e_1 and e_2 are the half-saturation constants for the functional responses of the blacktip shark to sardines and anchovies.
- m_1 and m_2 are the conversion rates of sardines and anchovies into predator biomass.
- d_1 is the natural mortality rate of the predator (blacktip shark).
- γ is the removal rate due to intraspecific competition within the predator population (blacktip sharks).

- E_1 and E_2 are the harvest coefficients for sardines and anchovies, respectively.

All parameters of this model are treated as positive constants. The first two equations represent the dynamics of the two prey species: sardines and anchovies, with the parameters accounting for natural growth rates, predation, and effects of fishing. The third equation models the population of predators (blacktip sharks) with account taken for the consumption of prey, natural mortality, and intra-specific competition among predators. This model of equations can be used to study the interactions between the prey species and predator species, namely sardines and anchovies with blacktip sharks, as well as the influence of competition, predation, and fishing.

The impact of including a nonzero harvesting rate within the prey equations from the predator-prey model, as well as environmental noise, is also discussed. It is assumed that random factors in the environment manifest as fluctuations in the intrinsic growth rates of the prey species and the mortality rate of the predator. Specifically, let a_1 and a_2 denote the intrinsic growth rates of sardines and anchovies and d_1 represent the mortality rate of the blacktip shark. These parameters are treated as average values with an additional error term. Using the central limit theorem, this error is modeled by a normal distribution and quantified by the difference between the current population sizes and their equilibrium state. The disturbances due to environmental noise are modeled as follows:

$$a_1 \to a_1 + \alpha_1 \dot{B}_1(t), \quad a_2 \to a_2 + \alpha_2 \dot{B}_2(t), \quad -d_1 \to -d_1 + \alpha_3 \dot{B}_3(t),$$

where α_1, α_2, and α_3 are the intensities of noise, and $\dot{B}_i(t)$ for $i = 1, 2, 3$ represents standard Brownian motion. These are characterized by:

$$\langle \dot{B}_i(t) \rangle = 0, \quad \text{for } i = 1, 2, 3,$$

and

$$\langle \dot{B}_k(t_k) \dot{B}_l(t_l) \rangle = \delta_{kl} \delta(t_k - t_l), \quad \text{for } k, l = 1, 2, 3,$$

where δ_{kl} is the Kronecker delta, and $\delta(\cdot)$ is the Dirac delta function.

The resulting stochastic model is formulated as:

$$\begin{aligned}
dx_1(t) &= x_1(t)\left[\big(a_1 - x_1(t)\big) - \frac{c_1 y(t)}{e_1 + x_1(t)} - E_1\right]dt + \alpha_1 x_1(t) dB_1(t), \\
dx_2(t) &= x_2(t)\left[\big(a_2 - x_2(t)\big) - \frac{c_2 y(t)}{e_2 + x_2(t)} - E_2\right]dt + \alpha_2 x_2(t) dB_2(t), \\
dy(t) &= y(t)\left[\frac{m_1 x_1(t)}{e_1 + x_1(t)} + \frac{m_2 x_2(t)}{e_2 + x_2(t)} - d_1 - \gamma y(t)\right]dt + \alpha_3 y(t) dB_3(t).
\end{aligned} \tag{2}$$

Every solution of the system (1) with positive initial conditions is an Itô process ([37], [38]). Without loss of generality, it is assumed that $\alpha_i > 0$ for $i = 1, 2, 3$.

The main goals of this study are:

1. To prove the stochastic stability of the model system around its positive equilibrium.
2. Investigate the existence and uniqueness of global solutions, which are helpful in studying the local and global dynamic behavior.

Thus, the goal is to find positive and global solutions of the system (1).

3 Stochastic Stability of the Positive Equilibrium

In this paper, the existence of the positive equilibrium $E^*(x_1^*, x_2^*, y^*)$ of the system (1) is checked. The system (1) must be considered equal to zero. This gives us two functions $f_1(x_1, x_2)$, $g_1(x_1, x_2)$. They then intersect at the equilibrium point $E^*(x_1^*, x_2^*, y^*)$. The following results from (1)

$$a_1 - x_1 - \frac{c_1 y}{e_1 + x_1} - E_1 = 0, \tag{3}$$

$$a_2 - x_2 - \frac{c_2 y}{e_2 + x_2} - E_2 = 0, \tag{4}$$

$$\frac{m_1 x_1}{e_1 + x_1} + \frac{m_2 x_2}{e_2 + x_2} - d_1 - \gamma y = 0. \tag{5}$$

From (3), (4) and (5) we get

$$y = \frac{(a_1 - x_1 - E_1)(e_1 + x_1)}{c_1}, \tag{6}$$

$$y = \frac{(a_2 - x_2 - E_2)(e_2 + x_2)}{c_2}, \tag{7}$$

$$y = \frac{1}{\gamma}[\frac{m_1 x_1}{e_1 + x_1} + \frac{m_2 x_2}{e_2 + x_2} - d_1]. \tag{8}$$

From (6) and (7) we find

$$f(x_1, x_2) = \frac{(a_1 - x_1 - E_1)(e_1 + x_1)}{c_1} - \frac{(a_2 - x_2 - E_2)(e_2 + x_2)}{c_2} = 0, \tag{9}$$

and from (6) and (8)

$$g(x_1, x_2) = \frac{(a_1 - x_1 - E_1)(e_1 + x_1)}{c_1} - \frac{1}{\gamma}[\frac{m_1 x_1}{e_1 + x_1} + \frac{m_2 x_2}{e_2 + x_2} - d_1]. \tag{10}$$

Equations (9) and (10) are two functions with two variables x_1, x_2. The existence of $E^*(x_1^*, x_2^*, y^*)$, must be shown, and the conditions under which $f(x_1, x_2)$ and $g(x_1, x_2)$ meet in the interior of the positive (x_1, x_2) plane at a point (x_1^*, x_2^*), must be found. (x_1^*, x_2^*), y^* can be obtained from (9).

From (9), x_2 tends to $x_2 f$ as $x_1^* \to 0$. x_{2f} is given by

$$x_{2f} = \frac{\hat{r_1} + \sqrt{\hat{r_1}^2 - 4\hat{r_2}}}{2}, \tag{11}$$

where $\hat{r_1} = (a_2 - e_2 - E_2)$, $\hat{r_2} = (a_1 - E_1)e_1\dfrac{c_2}{c_1} - (a_2 e_2 - E_2 e_2)$. x_{2f} is positive and real, provided $\hat{r_1}^2 > 4\hat{r_2}$.

From (10), as $x_1^* \to 0$, x_2^* tends to x_{2g} . x_{2g} is given by

$$x_2 f = \frac{\hat{r_3} e_2}{m_2 c_1 - \hat{r_3}}, \tag{12}$$

where $\hat{r_3} = (a_1 e_1 \gamma - e_1 \gamma E_1 + d_1 c_1)$. x_{2f} is positive and real, provided $m_2 c_1 + e_1 E_1 \gamma > a_1 e_1 \gamma + d_1 c_1$ and $a_1 > E_1$.

x_{2f} and x_{2f} are the points at which the functions $f(x_1, x_2)$ and $g(x_1, x_2)$ would cut the x_2 axis in the (x_1, x_2) plane, respectively. Then from (9), Since for $f(x_1, x_2)$, we have, $\dfrac{dx_2}{dx_1} > 0$ and for $g(x_1, x_2)$, we have $\dfrac{dx_2}{dx_1} < 0$, then $f(x_1, x_2)$ and $g(x_1, x_2)$ will meet if $x_{2f} < x_{2g}$.

Therefore, there is a positive equilibrium point $E^*(x_1^*, x_2^*, y^*)$ of the system (1).

Then we consider stochastic perturbations of the variables x_1, x_2, y around their values in positive equilibrium $E^*({x_1}^*, {x_2}^*, y^*)$. We investigate when it is feasible and locally asymptotically stable. The local stability of the stationary state E^* is implied by the existence condition of E^*. The stochastic model can therefore be expressed in the following form around its values at E^*

$$\begin{aligned}
dx_1(t) &= x_1(t)\left[\big(a_1 - x_1(t)\big) - \frac{c_1 y(t)}{e_1 + x_1(t)} - E_1\right]dt + \alpha_1(x_1 - {x_1}^*)dB_1(t),\\
dx_2(t) &= x_2(t)\left[\big(a_2 - x_2(t)\big) - \frac{c_2 y(t)}{e_2 + x_2(t)} - E_2\right]dt + \alpha_2(x_2 - {x_2}^*)dB_2(t),\\
dy(t) &= y(t)\left[\frac{m_1 x_1(t)}{e_1 + x_1(t)} + \frac{m_2 x_2(t)}{e_2 + x_2(t)} - d_1 - \gamma y(t)\right]dt + \alpha_3(y - y^*)dB_3(t).
\end{aligned} \tag{13}$$

The transformation is taken as

$$\widetilde{u}_1 = x_1 - {x_1}^*, \quad \widetilde{u}_2 = x_2 - {x_2}^*, \quad \widetilde{u}_3 = y - y^*. \tag{14}$$

Linearized SDEs around E^* take the form

$$d\widetilde{u}(t) = f(\widetilde{u}(t))dt + g(\widetilde{u}(t))dB, \tag{15}$$

where $\widetilde{u}(t) = (\widetilde{u}_1(t), \widetilde{u}_2(t), \widetilde{u}_3(t))^T$ and

$$f(\widetilde{u}(t)) = \begin{pmatrix} [-2x_1^* + \frac{c_1 {x_1}^* y^*}{(e_1 + {x_1}^*)^2}]\widetilde{u}_1(t) & 0 & -\frac{c_1 {x_1}^*}{(e_1 + {x_1}^*)}\widetilde{u}_3(t) \\ 0 & [-2x_2^* + \frac{c_2 {x_2}^* y^*}{(e_2 + {x_2}^*)^2}]\widetilde{u}_2(t) & -\frac{c_2 {x_2}^*}{(e_2 + {x_2}^*)}\widetilde{u}_3(t) \\ \frac{m_1 e_1 * y^*}{(e_1 + x_1^*)^2}\widetilde{u}_1(t) & \frac{m_2 e_2 y^*}{(e_2 + x_2^*)^2}\widetilde{u}_2(t) & -2\gamma y^* \widetilde{u}_3(t) \end{pmatrix}, \tag{16}$$

$$g(\widetilde{u}(t)) = \begin{pmatrix} \alpha_1 \widetilde{u}_1(t) & 0 & 0 \\ 0 & \alpha_2 \widetilde{u}_2(t) & 0 \\ 0 & 0 & \alpha_3 \widetilde{u}_3(t) \end{pmatrix}. \tag{17}$$

Since (15) the positive equilibrium E^* corresponds to the trivial solution $\widetilde{u}(t) = 0$. Let U' be the set. $U' = (t \geq t_0) \times R^n, t_0 \in R^+$. Hence $V \in C^0{}_2(U')$ is a twice continuously differentiable function with respect to $\widetilde{u}$ and a continuous function with respect to t. The following theorem, given in the book authored by Afanasev et al. [39], is stated.

Theorem 3.1. *Suppose there exists a function $U' = (t \geq t_0) \times R^n, t_0 \in R^+$ $V \in C^0{}_2(U')$ satisfying the inequalities*

$$K_1 |\widetilde{u}|^p \leq V(t, \widetilde{u}) \leq K_2 |\widetilde{u}|^p, \tag{18}$$

$$LV(t, \widetilde{u}) \leq -k_3 |\widetilde{u}|^p, \quad k_i > 0, \quad p > 0 \tag{19}$$

where $i = 1, 2, 3$. Then the trivial solution of (15) is exponentially p-stable, for $t \geq 0$.

In (19) and (18), if $p = 2$, then the trivial solution of (15) is exponentially mean-square stable. Then, the trivial solution of (15) is globally asymptotically stable in probability [40]. And

$$LV(t, \widetilde{u}) = \frac{\partial V(t, \widetilde{u})}{\partial t} + f^T(\widetilde{u}) \frac{\partial V(t, \widetilde{u})}{\partial \widetilde{u}} + \frac{1}{2} Trac[g^T(\widetilde{u}) \frac{\partial^2 V(t, \widetilde{u})}{\partial \widetilde{u}} g(\widetilde{u})],$$

where

$$\frac{\partial^2 V(t, \widetilde{u})}{\partial \widetilde{u}} = (\frac{\partial V}{\partial \widetilde{u}_1}, \frac{\partial V}{\partial \widetilde{u}_2}, \frac{\partial V}{\partial \widetilde{u}_3})^T,$$

$$\frac{\partial^2 V(t, \widetilde{u})}{\partial \widetilde{u}} = (\frac{\partial^2 V(t, \widetilde{u})}{\partial \widetilde{u}_i \partial \widetilde{u}_j}), \quad i, j = 1, 2, 3.$$

T is the transposition.

Theorem 3.2. *Suppose that* ${\alpha_1}^2 < 4x_1^* - \frac{2c_1{x_1}^*y^*}{(e_1+{x_1}^*)^2}$, ${\alpha_2}^2 > 4x_2^* - \frac{2c_2{x_2}^*y^*}{(e_2+{x_2}^*)^2}$, ${\alpha_3}^2 < 2\gamma y^*$. *Then the zero solution of (15) is asymptotically mean-square stable.*

Proof. Let consider the Lyapunov function,

$$V(\widetilde{u}) = \frac{1}{2}[\varpi_1\widetilde{u}_1^2 + \varpi_2\widetilde{u}_2^2 + \varpi_3\widetilde{u}_3^2], \tag{20}$$

where ϖ_i $(i = 1, 2, 3)$ are real positive constants to be chosen later. It is easy to check that inequalities (18) hold true with $p = 2$. Now

$$\begin{aligned} LV(u) = {} & \varpi_1\left[-2x_1^*\widetilde{u}_1(t) + \frac{c_1{x_1}^*y^*}{(e_1+{x_1}^*)^2}\widetilde{u}_1(t) - \frac{c_1{x_1}^*}{(e_1+{x_1}^*)}\widetilde{u}_3(t)\right]\widetilde{u}_1(t) \\ & + \varpi_2\left[-2x_2^*\widetilde{u}_2(t) + \frac{c_2{x_2}^*y^*}{(e_2+{x_2}^*)^2}\widetilde{u}_2(t) - \frac{c_2{x_2}^*}{(e_2+{x_2}^*)}\widetilde{u}_3(t)\right]\widetilde{u}_2(t) \\ & + \varpi_3\left[\frac{m_1e_1*y^*}{(e_1+x_1^*)^2}\widetilde{u}_1(t) + \frac{m_2e_2y^*}{(e_2+x_2^*)^2}\widetilde{u}_2(t) - 2\gamma y^*\widetilde{u}_3(t)\right]\widetilde{u}_3(t) \\ & + \frac{1}{2}Tr\left[g^T(\widetilde{u}(t))\frac{\partial^2V}{\partial\widetilde{u}^2}g(\widetilde{u}/(t))\right], \end{aligned} \tag{21}$$

where

$$g(\widetilde{u}(t)) = \begin{pmatrix} \alpha_1\widetilde{u}_1(t) & 0 & 0 \\ 0 & \alpha_2\widetilde{u}_2(t) & 0 \\ 0 & 0 & \alpha_3\widetilde{u}_3(t) \end{pmatrix}.$$

Hence

$$g^T(\widetilde{u}(t))\frac{\partial^2V}{\partial\widetilde{u}^2}g(\widetilde{u}(\tilde{t})) = \begin{pmatrix} \varpi_1{\alpha^2}_1\widetilde{u}_1^2(t) & 0 & 0 \\ 0 & \varpi_2{\alpha^2}_2\widetilde{u}_2^2(t) & 0 \\ 0 & 0 & \varpi_3{\alpha^2}_3\widetilde{u}_3^2(t) \end{pmatrix},$$

with

$$\frac{1}{2}Tr[g^T(\widetilde{u}(t))\frac{\partial^2V}{\partial\widetilde{u}^2}g(\widetilde{u}(\tilde{t}))] = \frac{1}{2}[\varpi_1{\alpha^2}_1\widetilde{u}_1^2 + \varpi_2{\alpha^2}_2\widetilde{u}_2^2 + \varpi_3{\alpha^2}_3\widetilde{u}_3^2]. \tag{22}$$

From (21) we select

$$\varpi_1\frac{c_1{x_1}^*}{(e_1+{x_1}^*)} = \varpi_3\frac{m_1c_1y^*}{(e_1+{x_1}^*)^2} \Rightarrow \varpi_1{x_1}^*(e_1+{x_1}^*) = \varpi_3m_1y^*,$$

and

$$\varpi_2 \frac{c_2 x_2{}^* y^*}{(e_2 + x_2{}^*)^2} = \varpi_3 \frac{m_1 e_1 * y^*}{(e_1 + x_1^*)^2} \Rightarrow \varpi_2 x_2{}^* (e_2 + x_2{}^*) = \varpi_3 m_2 y^*.$$

Then from (21) and (22) we get

$$LV = -(2x_1^* - \frac{c_1 x_1{}^* y^*}{(e_1 + x_1{}^*)^2} - \frac{\alpha_1{}^2}{2}) \varpi^2{}_1 \widetilde{u}_1^2$$

$$-(2x_2^* - \frac{c_2 x_2{}^* y^*}{(e_2 + x_2{}^*)^2} - \frac{\alpha_2{}^2}{2}) \varpi^2{}_2 \widetilde{u}_2^2$$

$$-(\gamma y^* - \alpha^2{}_3) \varpi_3{}^2 \widetilde{u}_3^2.$$

It follows that $LV \leq 0$ under the assumption of the **Theorem 3.2**. According to **Theorem 3.1** the proof, it is completed.

4 Existence and Uniqueness of the Global Positive Solution

Always, a stochastic differential equation has a unique global solution for every given initial value. The coefficients of the equation are required to satisfy the linear growth condition and the local Lipschitz condition [41, 42]. It is investigated whether the system (2) has a global positive solution, and it must be proven that the system has a suitable local solution by a suitable change of variables.

Theorem 4.1. *For any initial value* $(x_{10}, x_{20}, y_0) \in Int(\boldsymbol{R}_+^3)$*, the system (2) has unique positive local solution* $(x_1(t), x_2(t), y(t))$ *for* $t \in [0, \tau_e)$ *almost surely, where* τ_e *is the explosion time.*

The transformation is considered: $u_1(t) = logx_1(t)$, $u_2(t) = logx_2(t)$ and $v(t) = logy(t)$. By using Itô's formula, the system (2) becomes

$$\left.\begin{aligned} du_1(t) = &\quad [a_1 - E_1 - \tfrac{\alpha_1^2}{2} - e^{u_1(t)} - \tfrac{c_1 e^{v(t)}}{e_1 + e^{u_1(t)}}]dt + \alpha_1 dB_1(t), \\ du_2(t) = &\quad [a_2 - E_2 - \tfrac{\alpha_2^2}{2} - e^{u_2(t)} - \tfrac{c_2 e^{v(t)}}{e_2 + e^{u_2(t)}}]dt + \alpha_2 dB_2(t), \\ dv(t) = &\quad [\tfrac{m_1 e^{u_1(t)}}{e_1 + e^{u_1(t)}} + \tfrac{m_2 e^{u_2(t)}}{e_2 + e^{u_2(t)}} - d_1 - \gamma e^{v(t)} - \tfrac{\alpha_3^2}{2}]dt + \alpha_3 dB_3(t), \end{aligned}\right\} \quad (23)$$

subjected to the initial condition $u_1(0) = logx_1(0)$, $u_2(0) = logx_2(0)$ and $v(0) = logy(0)$. The drift part of the system (23) is expressed by the functions having linear growth which satisfy local Lipschitz condition. Hence there exists a unique local solution $(u_1(t), u_2(t), v(t))$ which is defined in some interval $[0, \tau_e)$, (τ_e is any finite positive real numbers). $x_1(t) = e^{u_1(t)}$, $x_2(t) = e^{u_2(t)}$, $y(t) = e^{v(t)}$ is unique positive local solution of the system (23) beginning from an interior point of the first quadrant. Now the aim is to examine that this local solution is actually the global solution of the system (23).

Further we have to show that $\tau_e = \infty$ almost surely, which will serve our purpose. First we explain the following lemma, see [42] and using this lemma we will prove the following theorem.

Lemma 4.1. *For all $z \in (0,\infty)$, $(z+4-2log2) \leq 2(z+1-logz)$ holds.*

Theorem 4.2. *For every initial condition $(x_{10}, x_{20}, y_0) \in$ Int(R^3_+), the system (2) holds a unique solution $(x_1(t), x_2(t), y(t))$ for $t \in [0,\infty)$ and the solution will remain in Int$(\boldsymbol{R}^3_+)$ with probability one.*

Proof. We take a sufficiently large positive integer $\hat{r}$ such that the interval $[\frac{1}{\hat{r}}, \hat{r}]$ contains (x_{10}, x_{20}, y_0). For every $r \geq r_0$ the stopping time τ_r is defined by,

$$\tau_t = \inf\{t \in [0,\tau_e) : x_1 \notin (\frac{1}{\hat{r}}, \hat{r}) \text{ or } x_2 \notin (\frac{1}{\hat{r}}, \hat{r}) \text{ or } y \notin (\frac{1}{\hat{r}}, \hat{r})\},$$

where $\inf \emptyset = \infty$ ($\emptyset$ being the empty set). Clearly, we see that τ_r is increasing as $r \to \infty$. Let $\tau_\infty = \lim_{r\to\infty} \tau_r$ then $\tau_\infty \leq \tau_e$ almost surely. We show that $\tau_\infty = \infty$ almost surely, which will eventually prove that $\tau_e = \infty$.

If possible, let $\tau_e \neq \infty$. Then there exist two constants $T > 0$ and $\epsilon \in (0,1)$ such that

$$P\{\tau_\infty \leq T\} > \epsilon. \tag{24}$$

In this case there is an integer $r_1 \geq r_0$ such that $\forall r \geq r_1$

$$P\{\tau_r \leq T\} \geq \epsilon. \tag{25}$$

Let us take V is a $\mathbf{C}^3$-function from Int$(\mathbf{R}^3_+) \to$ Int$(\mathbf{R}_+)$. Then

$$V(x_1,x_2,y) = \frac{m_1}{c_1}(x_1+1-logx_1) + \frac{m_2}{c_2}(x_2+1-logx_2) + (y+1-logy). \tag{26}$$

As $z+1-logz > 0, \forall z > 0$ the function $V(x_1,x_2,y)$ is positive-definite $\forall (x_1,x_2,y) \in$ Int$(\mathbf{R}^3_+)$. By applying Itô's formula and taking differential of $V(x_1,x_2,y)$ along the trajectories of equation (2), we obtain

$$dV(x_1,x_2,y) = LV(x_1,x_2,y)dt + \alpha_1(x_1-1)dB_1 + \alpha_2(x_2-1)dB_2 + \alpha_3(y-1)dB_3. \tag{27}$$

$$\begin{aligned} dV(x_1,x_2,y) = [&\frac{m_1}{c_1}(x_1-1)(a_1-E_1-x_1-\frac{c_1y}{e_1+x_1}) + \frac{m_2}{c_2}(x_2-1)(a_2-E_2-x_2-\frac{c_2y}{e_2+x_2}) \\ &+ (y-1)(-d_1-\gamma y+\frac{m_1x_1}{e_1+x_1}+\frac{m_2x_2}{e_2+x_2}) + \frac{m_1}{c_1}\frac{\alpha_1^2}{2} + \frac{m_2}{c_2}\frac{\alpha_2^2}{2} + \frac{\alpha_3^2}{2}]dt \\ &+ \alpha_1(x_1-1)dB_1 + \alpha_2(x_2-1)dB_2 + \alpha_3(y-1)dB_3. \end{aligned}$$

Since $x_1(t) > 0$, $x_2(t) > 0$ and $y(t) > 0$, we get

$$\begin{aligned} dV(x_1,x_2,y) \leq [&\frac{m_1}{c_1}(2a_1x_1-\frac{c_1x_1y}{e_1+x_1}) + \frac{m_2}{c_2}(2a_2x_2-\frac{c_2x_2y}{e_2+x_2}) + (d_1+\gamma y+\frac{m_1x_1y}{e_1+x_1}+\frac{m_2x_2y}{e_2+x_2}) \\ &+ \frac{m_1}{c_1}\frac{\alpha_1^2}{2} + \frac{m_2}{c_2}\frac{\alpha_2^2}{2} + \frac{\alpha_3^2}{2}]dt + \frac{m_1}{c_1}\alpha_1(x_1-1)dB_1 + \frac{m_2}{c_2}\alpha_2(x_2-1)dB_2 + \alpha_3(y-1)dB_3 \end{aligned}$$

$$\leq [\frac{2a_1m_1}{c_1}x_1 + \frac{2a_2m_2}{c_2}x_2 + d_1 + \gamma y + \frac{1}{2}(\frac{m_1\alpha_1^2}{c_1} + \frac{m_2\alpha_2^2}{c_2} + \alpha_3^2)]dt$$
$$+ \frac{m_1}{c_1}\alpha_1(x_1-1)dB_1 + \frac{m_2}{c_2}\alpha_2(x_2-1)dB_2 + \alpha_3(y-1)dB_3.$$

Using Lemma 4.1 we take

$$L_1 = d_1 + \frac{1}{2}\left(\frac{m_1\alpha_1^2}{c_1} + \frac{m_2\alpha_2^2}{c_2} + \alpha_3^2\right), L_2 = \max\left\{\frac{4a_1m_1}{c_1}, \frac{4a_2m_2}{c_2}, 2\gamma\right\}.$$

We have,

$$\begin{aligned}\frac{2a_1m_1}{c_1}x_1 + \frac{2a_2m_2}{c_2}x_2 + \gamma y &\leq \frac{4a_1m_1}{c_1}(x_1 + 1 - logx_1)\\ &+ \frac{2a_2m_2}{c_2}(x_2 + 1 - logx_2) + 2\gamma(y + 1 - logy)\\ &\leq L_2V(x_1, x_2, y).\end{aligned} \tag{28}$$

From (26) and (27) we get

$$dV(x_1, x_2, y) \leq \left[(L_2V(x_1, x_2, y) + L_1)dt + \frac{m_1}{c_1}\alpha_1(x_1-1)dB_1 + \frac{m_2}{c_2}\alpha_2(x_2-1)dB_2 + \alpha_3(y-1)dB_3\right].$$

Now we assume that $L_3 = \max\{L_1, L_2\}$ we have

$$dV(x_1, x_2, y) \leq L_3(V(x_1, x_2, y) + 1)dt + \frac{m_1}{c_1}\alpha_1(x_1-1)dB_1 + \frac{m_2}{c_2}\alpha_2(x_2-1)dB_2 + \alpha_3(y-1)dB_3.$$

Therefore, for $t_1 < T$

$$\begin{aligned}\int_0^{\tau_r\wedge t_1} dV(x_1, x_2, y) \leq L_3\int_0^{\tau_r\wedge t_1}(1 + V(x_1, x_2, y))dt + \frac{m_1\alpha_1}{c_1}\int_0^{\tau_r\wedge t_1}(x_1-1)dB_1\\ + \frac{m_2\alpha_2}{c_2}\int_0^{\tau_r\wedge t_1}(x_2-1)dB_2 + \alpha_3\int_0^{\tau_1\wedge t_1}(y-1)dB_3,\end{aligned}$$

where $\tau_r \wedge t_1 = \min\{\tau_r, t_1\}$. By applying the property of Itô integral [20] and from the above inequality we obtain

$$V(x_1(\tau_r\wedge t_1), x_2(\tau_r\wedge t_1), y(\tau_r\wedge t_1)) \leq V(x_{10}, x_{20}, y_0) + L_3E\int_0^{\tau_1\wedge t_1}(1 + V(x_1, x_2, y))dt.$$

Let us take expectation of both sides of the above inequality and use Fubini's theorem [43], we find

$$\begin{aligned}&\leq V(x_{10}, x_{20}, y_0) + L_3E\int_0^{\tau_r\wedge t_1}(1 + V(x_1, x_2, y))dt,\\ &= V(x_{10}, x_{20}, y_0) + L_3T + L_3\int_0^{t_1} EV(x_1(\tau_r\wedge t), x_2(\tau_r\wedge t), y(\tau_r\wedge t))dt.\end{aligned}$$

By applying Gronwall's inequality [44] we calculate from the above inequality

$$EV(x_1(\tau_r\wedge T), x_2(\tau_r\wedge T), y(\tau_r\wedge T)) \leq L_4, \tag{29}$$

where

$$L_4 = \Big(V(x_{10}, x_{20}, y_0)) + L_3 T\Big) e^{L_3 T}.$$

Set $\Omega_r = \{\tau_r \leq T\}$ for $r \geq r_1$ by (25) we find $P(\Omega_r) \geq \epsilon$. Since for any $\rho \in \Omega_r$, there is at least one of $x_1(\tau_r, \rho)$, $x_2(\tau_r, \rho)$, $y(\tau_r, \rho)$ which is equal either r or $\frac{1}{r}$. Hence $V(x_1(\tau_r), x_2(\tau_r), y(\tau_r))$ is no less than the smallest of $r + 1 - logr$ and $\frac{1}{r} + 1 + \log r$.

Consequently

$$V\big(x_1(\tau_r), x_2(\tau_r), y(\tau_r)\big) \geq (r + 1 - logr) \wedge (\frac{1}{r} + 1 + logr).$$

Thus from (24) and (29) it follows that

$$L_4 \geq E\Big[I_{\Omega_r}(\rho) V(x_1(\tau_r), x_2(\tau_r), y(\tau_r))\Big]$$

$$\geq \epsilon\Big[(r + 1 - logr) \wedge (\frac{1}{r} + 1 + logr)\Big],$$

where $I_{\Omega_r}(\rho)$ is the indicator function of Ω_r. If $r \to \infty$ we get $\infty > L_4 = \infty$. Which is a contradiction. So we must have $\tau_\infty = \infty$ almost surely. Hence proof is completed. □

5 Stochastic Persistence in the Mean

There are various concepts of stochastic persistence [45]. Here we apply the notion of stochastic persistence in mean. Stochastic persistence means, if we start from any arbitrary positive initial condition, that is, from any interior point of the first quadrant, the solution trajectories of the stochastic model persist within the interior of the first quadrant and remain bounded at all future time. In this section we have to examine the stochastic persistence of the model system (2) under certain parametric restriction(s). We define stochastic persistence in mean as follows.

The population $x(t)$ is said to be strongly persistent if $\langle x(t)\rangle_* > 0$, where

$$\langle x(t)\rangle := \frac{1}{t}\int_0^t x(s)ds, \qquad \langle x(t)\rangle_* := \liminf_{t\to+\infty} \frac{1}{t}\int_0^t x(s)ds.$$

Before we prove the main theorem, first we explain the following lemma [45]. The derivation of strong persistence conditions for system (2) is a direct consequence of the result stated in the following lemma.

Lemma 5.1. *Suppose* $x(t) \in \boldsymbol{C}[\Omega \times \boldsymbol{R}_+, \boldsymbol{R}_+^0]$, *where* $\boldsymbol{R}_+^0 = \{a | a > 0, a \in \boldsymbol{R}\}$.

i) If there exist positive constants ζ, T *and* $\sigma \geq 0$ *such that*

$$\ln x(t) \geq \sigma t - \zeta \int_0^t x(s)ds + \sum_{i=1}^n \beta_i B_i(t,)$$

for $t \geq T$, where β_i $(i = 1, 2, 3, ..., n)$ is constant, then $\langle x(t)\rangle_* \geq \frac{\sigma}{\zeta}$, almost surely.

ii) If there exist positive constants ζ, T and $\sigma \geq 0$ such that

$$\ln x(t) \leq \sigma t - \zeta \int_0^t x(s)ds + \sum_{i=1}^{n} \beta_i B_i(t,)$$

for $t \geq T$, where β_i $(i = 1, 2, 3, ..., n)$ is constant, then $\langle x(t)\rangle^* \leq \frac{\sigma}{\zeta}$, almost surely.

Definition 5.1. *$\langle x(t)\rangle^*$ is defined by*

$$\langle x(t)\rangle^* := \limsup_{t\to+\infty} \int_0^t x(s)ds.$$

Now we obtain the strong stochastic persistence result for the system (2) in the following theorem.

Lemma 5.2. *If $a_1 - E_1 - \frac{\alpha_1^2}{2} > 0$ and $a_2 - E_2 - \frac{\alpha_2^2}{2} > 0$, then every solution of the system satisfies*

$$\lim_{t\to+\infty} \langle x_1\rangle = a_1 - E_1 - \frac{\alpha_1^2}{2} \quad a.s. \quad and \quad \lim_{t\to+\infty} \langle x_2\rangle = a_2 - E_2 - \frac{\alpha_2^2}{2} \quad a.s.$$

$$m_1 + m_2 > d_1 + \frac{\alpha_3^2}{2} \quad and \quad \gamma > 0.$$

Using Itô's formula to the system (2) we find,

$$d(\ln(x_1(t))) = [(a_1 - x_1(t) - E_1 - c_1\frac{y(t)}{e_1 + x_1(t)} - \frac{\alpha_1^2}{2}]dt + \alpha_1 dB_1(t).$$

$$d(\ln(x_2(t))) = [(a_2 - x_2(t) - E_2 - c_2\frac{y(t)}{e_2 + x_2(t)} - \frac{\alpha_2^2}{2}]dt + \alpha_2 dB_2(t).$$

$$d(\ln(y(t))) = [-d_1 - \gamma y(t) + \frac{m_1 x_1(t)}{1 + e_1 x_1(t)} + \frac{m_2 x_2(t)}{e_2 + x_2(t)} - \frac{\alpha_3^2}{2}]dt + \alpha_3 dB_3(t)).$$

Integrating both sides from 0 to t and then dividing by t, we get

$$\frac{\ln[\frac{x_1(t)}{x_1(0)}]}{t} = (a_1 - E_1 - \frac{\alpha_1^2}{2}) - t^{-1}\int_0^t x_1(s)ds - c_1 t^{-1}\int_0^t \frac{y(s)}{e_1 + x_1(s)}ds + \alpha_1 t^{-1}B_1(t) \tag{30}$$

$$\frac{\ln[\frac{x_2(t)}{x_2(0)}]}{t} = (a_2 - E_2 - \frac{\alpha_2^2}{2}) - t^{-1}\int_0^t x_2(s)ds - c_2 t^{-1}\int_0^t \frac{y(s)}{e_2 + x_2(s)}ds + \alpha_2 t^{-1}B_2(t) \tag{31}$$

$$\frac{\ln[\frac{y(t)}{y(0)}]}{t} = (-d_1 - \frac{\alpha_3^2}{2}) - \gamma t^{-1}\int_0^t y(s)ds + m_1 t^{-1}\int_0^t \frac{x_1(s)}{e_1 + x_1(s)}ds + m_2 t^{-1}\int_0^t \frac{x_2(s)}{e_2 + x_2(s)}ds + \alpha_3 t^{-1}B_3(t). \tag{32}$$

By applying the Lemma 5.1 we have

$$\langle x_1(t)\rangle_* \geq [a_1 - E_1 - \frac{\alpha_1^2}{2}].$$

$$\langle x_2(t)\rangle_* \geq [a_2 - E_2 - \frac{\alpha_2^2}{2}].$$

$$\langle y(t)\rangle_* \geq \frac{-d_1 - \frac{\alpha_3^2}{2} + m_1 + m_2}{\gamma}.$$

Therefore, $\langle x_1(t)\rangle_* \geq 0$, $\langle x_2(t)\rangle_* \geq 0$ and $\langle y(t)\rangle_* \geq 0$, whenever $a_1 \geq E_1 + \frac{\alpha_1^2}{2}$, $a_2 \geq E_2 + \frac{\alpha_2^2}{2}$ and $m_1 + m_2 > d_1 + \frac{\alpha_3^2}{2}$ and $\gamma > 0$. Hence the required results are obtained.

The strong persistence results of the predator-prey model under consideration within fluctuating environment absolutely count on the intensity of environmental fluctuation. The threshold values of environmental driving forces are $\alpha_1^* \equiv \sqrt{2(a_1 - E_1 - c_1)}$, $\alpha_2^* \equiv \sqrt{2(a_2 - E_2 - c_2)}$ and $\alpha_3^* \equiv \sqrt{2(m_1 + m_2 - d_1)}$. Sometimes situations occur that species population are going to extinction.

Case 1. The prey species with lower growth rate becomes extinct if intensities of environmental fluctuations α_1^*, α_2^* are quite high whereas α_3^* is negligible quantity.

Case 2. Predator population goes to extinction if α_1^*, α_2^* and α_3^* are extremely high.

It have been seen that under some specific conditions, population neither explode nor goes to extinction whenever fluctuation intensities of environmental driving forces are below the threshold limits.

6 Stationary Distribution and Fokker–Planck Analysis

Here we try to establish the existence of stationary distribution of system (2). If stationary distribution of populations exists then that ensure the stability of the system in stochastic meaner. Before we prove the main theorem related with the stationary distribution, first we explain the following result regarding the existence of unique interior equilibrium of the original deterministic system, which have to use to show the main theorem of this section.

Lemma 6.1. *Let* $\mathbf{E}_l$ *be the* l*-dimensional Euclidean space and* $X(t)$ *be a homogeneous Markov process and it is defined in* $\mathbf{E}_l$*. Let* $X(t)$ *be denoted by the following system of stochastic differential equations:*

$$dX(t) = b(X(t))dt + \sum_{k=1}^{r} f_k(X)dB_k(t). \tag{33}$$

The diffusion matrix $A(x)$ *is defined by [6],*

$$A(x) = \big(b_{ij}(x)\big),$$

where $b_{ij}(x) = \sum_{k=1}^{r} \alpha_k^i(x)\alpha_k^j(x)$.

Assuming there is a bounded domain $S \subset \boldsymbol{E}_l$ with regular boundary Γ with the following properties,

H1: In the domain S and some neighborhood thereof, the smallest eigenvalue of the diffusion matrix $A(x)$ is bounded away from zero.

H2: If $x \in \boldsymbol{E}_l - S$, the mean time τ at which a path emerging from x reaches the set S is finite, and $\sup_{x\in S_1} \boldsymbol{E}_x\tau < \infty$, for every compact subset S_1.

Lemma 6.2. *If above assumptions hold, then the Markov process* $X(t)$ *has a stationary distribution* $\sigma(.)$*. Let* $g(.)$ *be a function integrable with respect to the measure* σ*. Then* $\forall x \in \boldsymbol{E}_l$*,*

$$P_x\{\lim_{T\to\infty} \frac{1}{T}\int_0^t g(X(t))dt = \int_{\boldsymbol{E}_l} g(x)\sigma(dx)\} = 1.$$

Remark 6.1. *The proof of Lemma 6.2 can be found in [45]. A stationary distribution with a suitable density function exists (see Theorem 5.1 and Lemma 9.4 in [46]); see also our result in Lemma 6.2.*

To verify assumption (H1), it suffices to check that the operator F *is uniformly elliptic in* S*, where*

$$F_{u'} = b(x)\cdot u'_x + \frac{\mathrm{tr}(A(x))\cdot u''_{xx}}{2}.$$

This condition implies the existence of a constant $M > 0$ *such that*

$$\sum_{i,j=1}^{r} b_{ij}(x)\,\xi_i\xi_j \geq M|\xi|^2, \quad \text{for all } x \in S,\ \xi \in \mathbb{R}^r,$$

as discussed in [47].

To validate assumption (H2), we must show that there exists a neighborhood $S \subset \mathbb{E}_l$ *and a non-negative* $\mathcal{C}^3$*-function* V *such that* $\mathcal{L}V(x)$ *is negative definite for every* $x \in \mathbb{E}_l \setminus S$*; see [40].*

The system (2) can be expressed of the following form :

$$\begin{aligned} d\begin{pmatrix} x_1(t) \\ x_2(t) \\ y(t) \end{pmatrix} &= \begin{pmatrix} x(t)(a_1 - x_1(t)) - c_1\frac{x_1(t)y(t)}{e_1+x_1(t)} - E_1x_1(t) \\ x_2(t)(a_2 - x_2(t)) - c_2\frac{x_2(t)y(t)}{e_2+x_2(t)} - E_2x_2(t) \\ y(t)[\frac{m_1x_1(t)}{e_1+x_1(t)} + \frac{m_2x_2(t)}{e_2+x_2(t)} - d_1 - \gamma y(t)] \end{pmatrix} dt \\ &+ \begin{pmatrix} \alpha_1x_1(t) \\ 0 \\ 0 \end{pmatrix} dB_1(t) + \begin{pmatrix} 0 \\ \alpha_2x_2(t) \\ 0 \end{pmatrix} dB_2(t) + \begin{pmatrix} 0 \\ 0 \\ \alpha_3y(t) \end{pmatrix} dB_3(t) \end{aligned} \tag{34}$$

where diffusion matrix is given by,

$$A(x) = \begin{pmatrix} \alpha_1^2x_1^2 & 0 & 0 \\ 0 & \alpha_2^2x_2^2 & 0 \\ 0 & 0 & \alpha_3^2y^2 \end{pmatrix}. \tag{35}$$

Now in the following theorem we have to show the existence of a stationary distribution $\sigma(.)$ for the system (2).

Theorem 6.1. *Assume the following conditions hold:*

- $\tilde{D}_1e_1 - c_1y^* > 0$,
- $\tilde{D}_2e_2 - c_2y^* > 0$,
- $\delta < \min\left[\left(M_2 - \frac{M_5}{2\epsilon}\right)(x_1^*)^2,\ \left(M_3 - \frac{M_6}{2\epsilon}\right)(x_2^*)^2,\ \left(M_2 - \frac{(M_5+M_6)\epsilon}{2}\right)(y^*)^2\right]$,

where (x_1^*, x_2^*, y^*) is the positive equilibrium of system (2), and

$$\tilde{D}_1 = e_1 + x_1^*, \quad \tilde{D}_2 = e_2 + x_2^*$$

$$\delta = \left(M_2 - \frac{M_5}{2\epsilon}\right)(x_1 - x_1^*)^2 + \left(M_3 - \frac{M_6}{2\epsilon}\right)(x_2 - x_2^*)^2 + \left(M_2 - \frac{(M_5+M_6)\epsilon}{2}\right)(y - y^*)^2$$

The constants are defined as:

$$M_1 = M_1'e_1e_2, \quad M_2 = e_2(\tilde{D}_1e_1 - c_1y^*), \quad M_3 = e_1(\tilde{D}_2e_2 - c_2y^*),$$

$$M_4 = \gamma\tilde{D}_1\tilde{D}_2e_1e_2, \quad M_5 = (c_1\tilde{D}_1 + m_1\tilde{D}_2x_1^* + m_1\tilde{D}_1\tilde{D}_2)e_2,$$

$$M_6 = (c_2\tilde{D}_2 + m_2\tilde{D}_1x_2^* + m_2\tilde{D}_1\tilde{D}_2)e_1,$$

$$M_1' = \frac{\tilde{D}_1}{2}x_1^*\alpha_1^2 + \frac{\tilde{D}_2}{2}x_2^*\alpha_2^2 + \frac{\tilde{D}_1\tilde{D}_2}{2}\alpha_3^2y^*.$$

Furthermore, $\epsilon > 0$ such that:

$$M_2 - \frac{M_5}{2\epsilon} > 0, \quad M_3 - \frac{M_6}{2\epsilon} > 0, \quad M_2 - \frac{(M_5+M_6)\epsilon}{2} > 0$$

hold simultaneously.

Proof. The system (2) has a unique positive interior equilibrium (x_1^*, x_2^*, y^*). Then we have $x_1^* + \frac{c_1 y^*}{e_1+x_1^*} = a_1 - E_1$, $x_2^* + \frac{c_2 y^*}{e_2+x_2^*} = a_2 - E_2$, $\tilde{D}_1 = e_1 + x_1$ and $\tilde{D}_2 = e_2 + x_2$.

Considering the positive definite function as follows $V : \boldsymbol{E}_3 \to \mathbf{R}_+$ where $\boldsymbol{E}_3 = \text{Int}\mathbf{R}_+^3$ as follows

$$V(x_1, x_2, y) = \tilde{D}_1(x_1 + 1 - \ln(\frac{x_1}{x_1^*})) + \tilde{D}_2(x_2 + 1 - \ln(\frac{x_2}{x_2^*})) + \tilde{D}_1\tilde{D}_2(y + 1 - \ln(\frac{y}{y^*})).$$

Then by applying Itô's formula, we obtain

$$\begin{aligned} dV(x_1, x_2, y) &= dV_1(x_1, x_2, y) + dV_2(x_1, x_2, y) + dV_3(x_1, x_2, y) \\ &= L_5V(x_1, x_2, y)dt + \alpha_1\tilde{D}_1(x_1 - x_1^*)dB_1 + \alpha_1\tilde{D}_2(x_2 - x_2^*)dB_2 + \alpha_3\tilde{D}_1\tilde{D}_2(y - y^*)dB_1, \end{aligned}$$

where

$$\begin{aligned} L_5V(x_1, x_2, y) &= [-\{\tilde{D}_1 - \frac{y^*c_1}{e_1 + x_1}\}(x_1 - x_1^*)^2 - \{\tilde{D}_2 - \frac{y^*c_2}{e_2 + x_2}\}(x_2 - x_2^*)^2 - \gamma\tilde{D}_1\tilde{D}_2(y - y^*)^2 \\ &\quad - \frac{c_1\tilde{D}_1(x_1 - x_1^*)(y - y^*)}{e_1 + x_1} - \frac{c_2\tilde{D}_2(x2 - x_2^*)(y - y^*)}{e_2 + x_2} + \frac{m_1\tilde{D}_1\tilde{D}_2(x_1 - x_1^*)(y - y^*)}{e_1 + x_1} \\ &\quad + \frac{m_2\tilde{D}_2(x_2 - x_2^*)(y - y^*)}{e_2 + x_2} - \frac{m_1\tilde{D}_2x_1^*(x_1 - x_1^*)(y - y^*)}{e_1 + x_1} - \frac{m_2\tilde{D}_1x_2^*(x_2 - x_2^*)(y - y^*)}{e_2 + x_2} + \frac{\tilde{D}_1}{2}x_1^*\alpha_1^2 \\ &\quad + \frac{\tilde{D}_2}{2}x_2^*\alpha_2^2 + \frac{\tilde{D}_1\tilde{D}_2}{2}\alpha_3^2y^*]dt + \alpha_1\tilde{D}_1(x_1 - x_1^*)dB_1 + \alpha_2\tilde{D}_2(x_2 - x_2^*)dB_2 + \tilde{D}_1\tilde{D}_2\alpha_3(y - y^*)dB_3 \\ &\leq [-\tilde{D}_1(x_1 - x_1^*)^2 - \tilde{D}_2(x_2 - x_2^*)^2 - \gamma\tilde{D}_1\tilde{D}_2(y - y^*)^2 - \frac{c_1\tilde{D}_1(x_1 - x_1^*)(y - y^*)}{e_1 + x_1} \\ &\quad - \frac{c_2\tilde{D}_2(x2 - x_2^*)(y - y^*)}{e_2 + x_2} + \frac{m_1\tilde{D}_1\tilde{D}_2(x_1 - x_1^*)(y - y^*)}{e_1 + x_1} + \frac{\tilde{D}_1}{2}x_1^*\alpha_1^2 \\ &\quad - \frac{m_1\tilde{D}_2x_1^*(x_1 - x_1^*)(y - y^*)}{(e_1 + x_1)} + \frac{m_2\tilde{D}_1\tilde{D}_2(y - y^*)(x_2 - x_2^*)}{e_2 + x_2} - \frac{m_2\tilde{D}_1x_2^*(x_2 - x_2^*)(y - y^*)}{(e_2 + x_2)} \\ &\quad + \frac{c_1y^*(x_1 - x_1^*)^2}{e_1 + x_1} + \frac{c_2y^*(x_2 - x_2^*)^2}{e_2 + x_2} + M_1', \end{aligned}$$

where

$$M_1' = \frac{\tilde{D}_1}{2}x_1^*\alpha_1^2 + \frac{\tilde{D}_2}{2}x_2^*\alpha_2^2 + \frac{\tilde{D}_1\tilde{D}_2}{2}\alpha_3^2y^*.$$

Then

$$\begin{aligned} L_5V(x_1, x_2, y) &\leq -\tilde{D}_1(x_1 - x_1^*)^2 - \tilde{D}_2(x_2 - x_2^*)^2 - \gamma\tilde{D}_1\tilde{D}_2(y - y^*)^2 + |x_1 - x_1^*||y - y^*|[\frac{c_1\tilde{D}_1}{e_1 + x_1} + \frac{m_1\tilde{D}_2x_1^*}{e_1 + x_1} \\ &\quad + \frac{m_1\tilde{D}_1\tilde{D}_2}{e_1 + x_1}] + |x_2 - x_2^*||y - y^*|[\frac{c_2\tilde{D}_1}{e_2 + x_2} + \frac{m_2\tilde{D}_1x_2^*}{e_2 + x_2} + \frac{m_2\tilde{D}_1\tilde{D}_2}{e_2 + x_2}] \end{aligned}$$

$$+\frac{c_1y^*(x_1-x_1^*)^2}{e_1+x_1}+\frac{c_2y^*(x_2-x_2^*)^2}{e_2+x_2}+M_1^{'}$$
$$\leq -(\tilde{D}_1-\frac{c_1y^*}{e_1})(x_1-x_1^*)^2-(\tilde{D}_2-\frac{c_2y^*}{e_2})(x_2-x_2^*)^2-\gamma\tilde{D}_1\tilde{D}_2(y-y^*)^2$$
$$+|x_1-x_1^*||y-y^*|\frac{(c_1\tilde{D}_1+m_1\tilde{D}_2x_1^*+m_1\tilde{D}_1\tilde{D}_2)}{e_1}$$
$$+|x_2-x_2^*||y-y^*|\frac{(c_2\tilde{D}_2+m_2\tilde{D}_1x_2^*+m_2\tilde{D}_1\tilde{D}_2)}{e_2}+M_1^{'}$$

$$e_1e_2L_5V(x_1,x_2,y)\leq -e_2(\tilde{D}_1e_1-c_1y^*)(x_1-x_1^*)^2-e_1(\tilde{D}_2e_2-c_2y^*)(x_2-x_2^*)^2$$
$$-\gamma\tilde{D}_1\tilde{D}_2e_1e_2(y-y^*)^2+(c_1\tilde{D}_1+m_1\tilde{D}_2x_1^*+m_1\tilde{D}_1\tilde{D}_2)e_2|x_1-x_1^*||y-y^*|$$
$$+(c_2\tilde{D}_2+m_2\tilde{D}_1x_2^*+m_2\tilde{D}_1\tilde{D}_2)e_1|x_2-x_2^*||y-y^*|+M_1^{'}e_1e_2.$$

Let

$$M_1=M_1^{'}e_1e_2,\quad M_2=e_2(\tilde{D}_1e_1-c_1y^*),\quad M_3=e_1(\tilde{D}_2e_2-c_2y^*),\quad M_4=\gamma\tilde{D}_1\tilde{D}_2e_1e_2,$$

$$M_5=(c_1\tilde{D}_1+m_1\tilde{D}_2x_1^*+m_1\tilde{D}_1\tilde{D}_2)e_2,\quad \text{and}\quad M_6=(c_2\tilde{D}_2+m_2\tilde{D}_1x_2^*+m_2\tilde{D}_1\tilde{D}_2)e_1.$$

Then above expression converts into

$$L_6V(x_1,x_2,y)\leq -M_2(x_1-x_1^*)^2-M_3(x_2-x_2^*)^2-M_4(y-y^*)^2+M_5|x_1-x_1^*||y-y^*|+M_6|x_2-x_2^*||y-y^*|+M_1.$$

Then by Young's inequality, we find

$$M_5|x_1-x_1^*||y-y^*|\leq M_5[\frac{(x_1-x_1^*)^2}{2\epsilon}+\frac{\epsilon(y-y^*)^2}{2}],$$

and

$$M_6|x_2-x_2^*||y-y^*|\leq M_6[\frac{(x_2-x_2^*)^2}{2\epsilon}+\frac{\epsilon(y-y^*)^2}{2}].$$

Therefore,

$$L_6V(x_1,x_2,y)\leq -M_2(x_1-x_1^*)^2-M_3(x_2-x_2^*)^2-M_4(y-y^*)^2+M_5[\frac{(x_1-x_1^*)^2}{2\epsilon}+\frac{\epsilon(y-y^*)^2}{2}]$$
$$+M_6[\frac{(x_2-x_2^*)^2}{2\epsilon}+\frac{\epsilon(y-y^*)^2}{2}]+M_1,$$
$$\leq -(M_2-\frac{M_5}{2\epsilon})(x_1-x_1^*)^2-(M_3-\frac{M_6}{2\epsilon})(x_2-x_2^*)^2-(M_4-\frac{(M_5+M_6)\epsilon}{2})(y-y^*)^2+\delta.$$

If δ satisfies the following condition,

$$\delta < \min\{(M_2 - \frac{M_5}{2\epsilon})(x_1^*)^2, (M_3 - \frac{M_6}{2\epsilon})(x_2^*)^2, (M_2 - \frac{(M_5+M_6)\epsilon}{2})(y^*)^2\},$$

then the ellipsoid

$$\delta = (M_2 - \frac{M_5}{2\epsilon})(x_1 - x_1^*)^2 + (M_3 - \frac{M_6}{2\epsilon})(x_2 - x_2^*)^2 + (M_2 - \frac{(M_5+M_6)\epsilon}{2})(y - y^*)^2,$$

lies entirely within int $\mathbf{R}^3$. We select S to be the neighborhood of the elliptic region with $S \subseteq \boldsymbol{E}_3 =$ int $\mathbf{R}^3$, where $\bar{S}$ is the compact closure of S. So for $x \in S - \boldsymbol{E}_3, LV < 0$ which is implied that condition H2 in the **Lemma 6.1** is satisfied.

Besides, $M_1^{'} = \min\{\alpha_1^2 x_1^2, \alpha_2^2 x_2^2, \alpha_3^2 y^2 : (x_1, x_2, y) \in \bar{S})\} > 0$, such that

$$\sum_{i,j=1}^{3} b_{ij}\xi_i\xi_j = \alpha_1^2 x_1^2 \xi_1^2 + \alpha_2^2 x_2^2 \xi_2^2 + \alpha_3^2 y^2 \xi_3^2 \geq M|\xi|^2,$$

for $(x_1, x_2, y) \in \bar{S}$ and $\xi \in \mathbf{R}^3$, which shows that condition H1 of Lemma 6.2 is also satisfied. Thus, the system (2) has a stationary distribution $\sigma(.)$. □

7 Numerical Simulation

In this section, we provide numerical simulations to support the analytical findings of the model system. The system (2) is simulated using MATLAB with the following parameter values:

Table 1: Parameter values and their descriptions for the model.

Parameter	**Value**	**Description**
a_1	0.15	Growth rate of prey 1 (sardines)
a_2	0.4	Growth rate of prey 2 (anchovies)
e_1	1000	Half-saturation constant for x_1
e_2	1500	Half-saturation constant for x_2
c_1	0.07	Predation rate on x_1
c_2	0.06	Predation rate on x_2
m_1	0.05	Predator's gain from x_1
m_2	0.04	Predator's gain from x_2
E_1	0.05	Harvesting rate of sardines
E_2	0.05	Harvesting rate of anchovies
d_1	0.02	Predator natural death rate
γ	0.03	Predator density-dependent mortality
$\alpha_1, \alpha_2, \alpha_3$	0.1	Noise intensities

The selected parameter values aim to realistically replicate the ecological dynamics of the California Current, where two prey species—*sardines* (*Sardinops sagax*) and *anchovies* (*Engraulis mordax*)—are subjected to continuous harvesting, while the predator, such as the *blacktip shark*, relies on both species for sustenance. The intrinsic growth rates, $a_1 = 0.15$ for sardines and $a_2 = 0.4$ for anchovies, reflect biological productivity, with anchovies exhibiting a faster reproductive cycle. The half-saturation constants $e_1 = 1000$ and $e_2 = 1500$ characterize the nonlinear Holling Type-II functional response, which captures how prey availability affects predator consumption rates.

The predation coefficients $c_1 = 0.07$ and $c_2 = 0.06$ indicate slightly stronger predation on sardines, likely due to their schooling behavior. Harvesting rates $E_1 = E_2 = 0.05$ correspond to levels observed in heavily exploited fisheries. Predator mortality is modeled via a natural death rate $d_1 = 0.02$ and a density-dependent term $\gamma = 0.03$, accounting for intraspecific competition. The stochastic terms $\alpha_1 = \alpha_2 = \alpha_3 = 0.1$ represent environmental variability, such as temperature fluctuations and resource uncertainty. These parameters are informed by empirical data from the California Current Large Marine Ecosystem (CCLME), spanning 2000–2015, sourced from NOAA and the Pacific Fishery Management Council. Notably, uncertainties in shark population estimates due to migration and sparse sampling may affect predation accuracy.

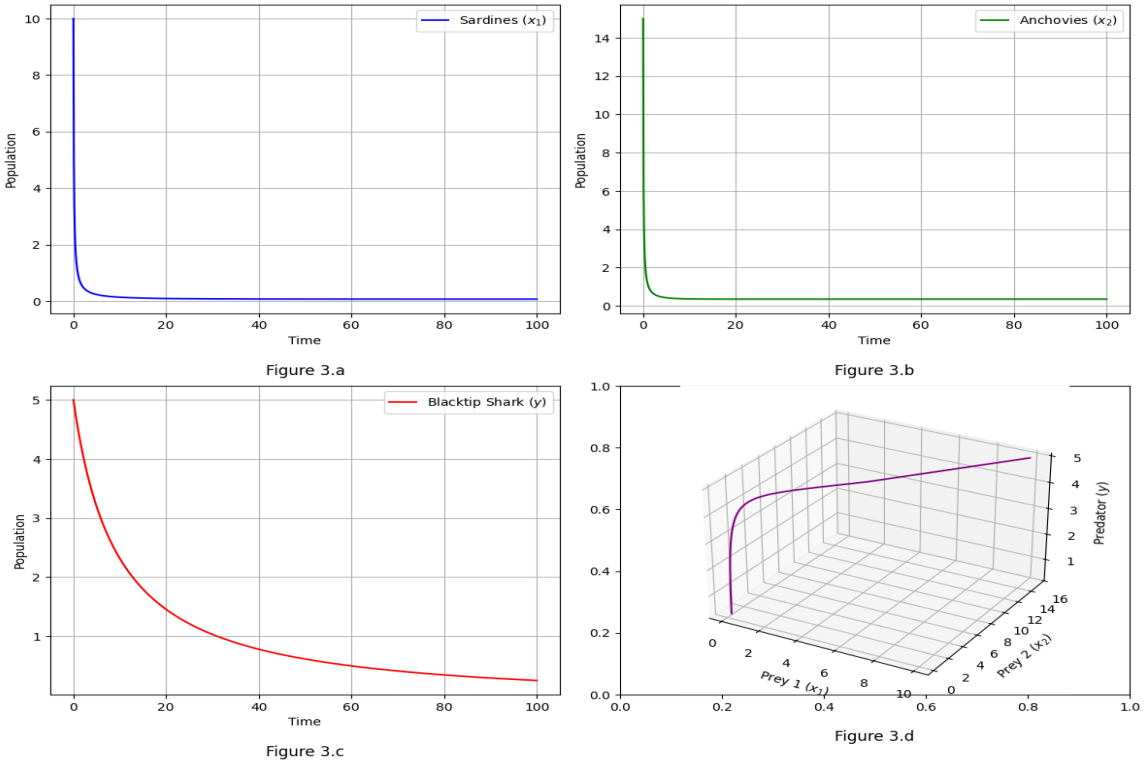

Figure 1: (a) Oscillation of $x_1(t)$ population (sardines), (b) Oscillation of $x_2(t)$ population (anchovies), (c) Extinction of $y(t)$ population (blacktip shark) for $\alpha_1 = 0$, $\alpha_2 = 0$, $\alpha_3 = 0$ with parameters from Table 1.

Figure 1 presents the deterministic dynamics in the absence of noise. The predator population y depends on the consumption of both prey species, whereas the prey populations x_1 and x_2 grow autonomously when unimpacted by predation. The system exhibits five equilibrium points: the trivial state $(0, 0, 0)$, single-prey states $(0.10, 0, 0)$ and $(0, 0.35, 0)$, a prey-only coexistence $(0.10, 0.35, 0)$, and a biologically feasible coexistence equilibrium $(614.29, 1298.08, 0.27)$. The previously proposed point $(0.10, 0.35, -0.5)$ was discarded due to the non-physical negative predator biomass.

Simulations initiated at $(500, 1000, 0.5)$ over $t \in [0, 1000]$ confirm convergence to the coexistence equilibrium, verifying its local stability in the deterministic case. This result affirms the ecological realism of the model and motivates further exploration of system behavior under stochastic perturbations.

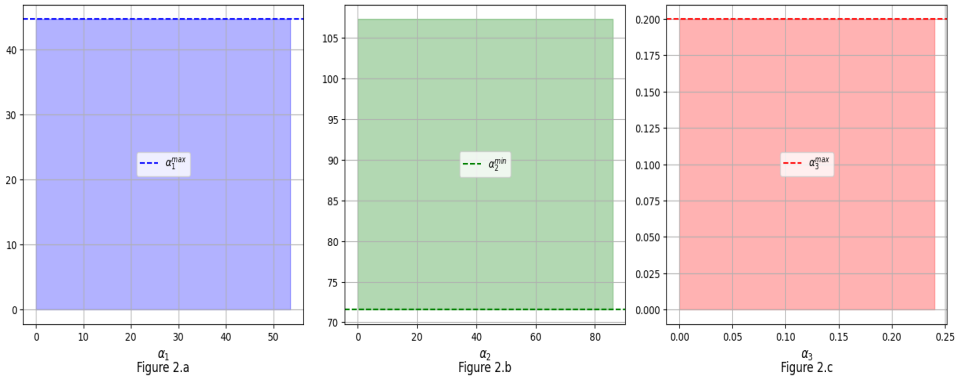

Figure 2: (a) Valid region for α_1 ($0 < \alpha_1 < 49.57$), (b) Valid region for α_2 ($\alpha_2 > 72.06$), (c) Valid region for α_3 ($0 < \alpha_3 < 0.127$), based on stability analysis of the coexistence equilibrium and parameters from Table 1.

Building on the simulation results, the noise intensities α_1, α_2, and α_3 represent environmental fluctuations acting on the sardine (x_1), anchovy (x_2), and predator (y) populations, respectively. To ensure biologically realistic behavior—such as non-negative population densities and bounded oscillations—these stochastic perturbations must lie within specific ranges. Numerical analysis around the coexistence equilibrium $(614.29, 1298.08, 0.27)$, using parameters from Table 1, reveals the constraints: $0 < \alpha_1 < 49.57$, $\alpha_2 > 72.06$, and $0 < \alpha_3 < 0.127$, as shown in Figure 2.

These stability regions serve as critical thresholds, beyond which the system may experience extinction or unbounded fluctuations. Notably, increasing α_2—the intensity of environmental noise on anchovies—beyond 72.06 appears to stabilize the system, likely due to compensatory mechanisms in anchovy population dynamics. This finding contrasts with the destabilizing effects of increasing α_1 (sardines) and α_3 (predator).

The baseline noise values $\alpha_1 = \alpha_2 = \alpha_3 = 0.1$ lie well within the safe bounds, promoting long-term coexistence. However, when these values are significantly increased—for instance, to $\alpha_1 = 3.0$, $\alpha_2 = 3.0$, $\alpha_3 = 2.5$—the system enters an unstable regime, as shown in subsequent simulations (Figure 4). Such parameter regimes may lead to predator extinction and chaotic fluctuations in prey populations, emphasizing the importance of environmental noise regulation.

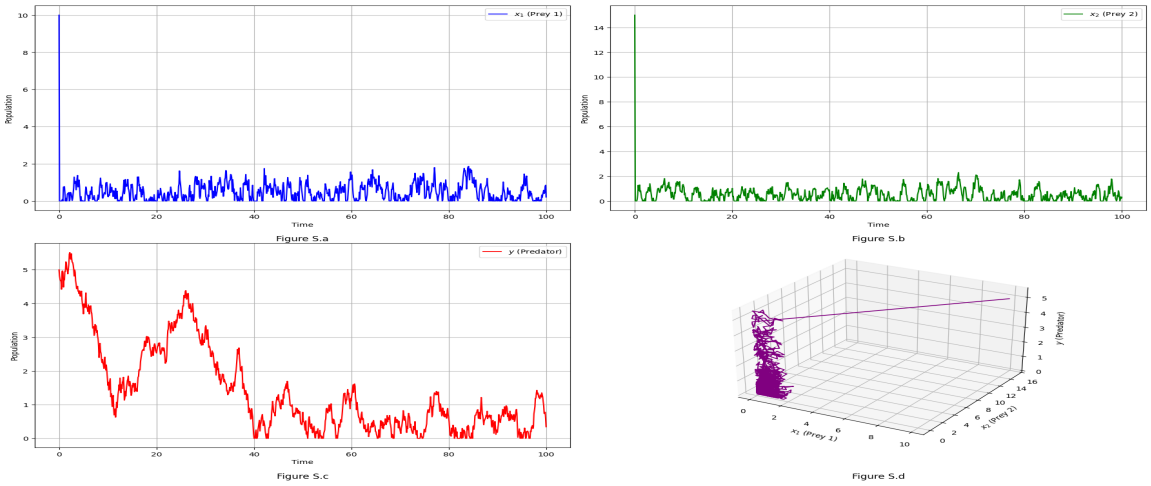

Figure 3: (a) Oscillation of $x_1(t)$ (sardines), (b) Oscillation of $x_2(t)$ (anchovies), (c) Oscillation and extinction of $y(t)$ (blacktip shark), (d) 3D phase trajectory of the system for $\alpha_1 = 1.0$, $\alpha_2 = 1.0$, $\alpha_3 = 0.5$ using parameters from Table 1.

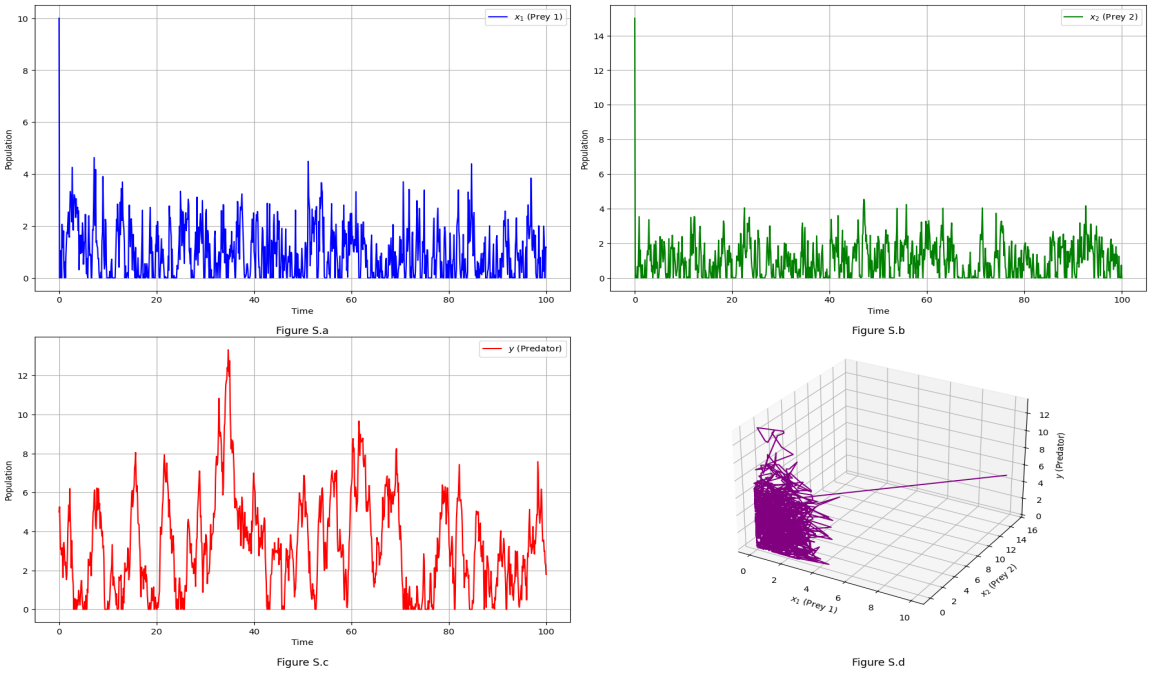

Figure 4: (a) Long-term oscillation of $x_1(t)$ (sardines), (b) Long-term oscillation of $x_2(t)$ (anchovies), (c) Oscillation and extinction of $y(t)$ (blacktip shark), (d) 3D phase trajectory of the system for $\alpha_1 = 3.0$, $\alpha_2 = 3.0$, $\alpha_3 = 2.5$ using parameters from Table 1.

Figure 3 demonstrates system dynamics under moderate noise intensities. Subfigures (a) and (b) show the prey populations (x_1 and x_2) oscillating around their respective equilibrium values, with mild irregularities introduced by the noise. The sardine population fluctuates around $x_1 \approx 614.29$ and anchovies around $x_2 \approx 1298.08$, consistent with their biological growth and interaction parameters.

In subfigure (c), the predator population y initially oscillates but eventually declines to extinction around $t = 800$. This is attributed to the noise intensity $\alpha_3 = 0.5$, which exceeds the upper bound of the stability region ($\alpha_3 < 0.127$), destabilizing the predator's persistence. The corresponding 3D phase portrait in subfigure (d) illustrates a spiraling trajectory that ultimately collapses onto the x_1–x_2 plane, confirming predator extinction and continued prey coexistence.

In contrast, Figure 4 explores the case of high noise intensities, where α_1, α_2, and α_3 all exceed their respective stability bounds (except α_1, which remains within tolerance). The prey populations (subfigures a and b) display chaotic and amplified oscillations, particularly for anchovies (x_2), whose associated noise $\alpha_2 = 3.0$ falls below the required stabilizing threshold ($\alpha_2 > 72.06$). The predator population (subfigure c) rapidly declines, going extinct well before $t = 100$, a direct result of excessive noise in the predator mortality term. The 3D trajectory in subfigure (d) shows a chaotic path diverging from the coexistence equilibrium, followed by collapse as the predator vanishes.

These simulations affirm that noise intensity plays a pivotal role in shaping ecological dynamics. Moderate stochasticity allows prey persistence while threatening predator survival; extreme noise levels destabilize the entire system. The validity of the stability bounds shown in Figure 2 is thus confirmed, reinforcing the ecological importance of maintaining environmental conditions within safe thresholds.

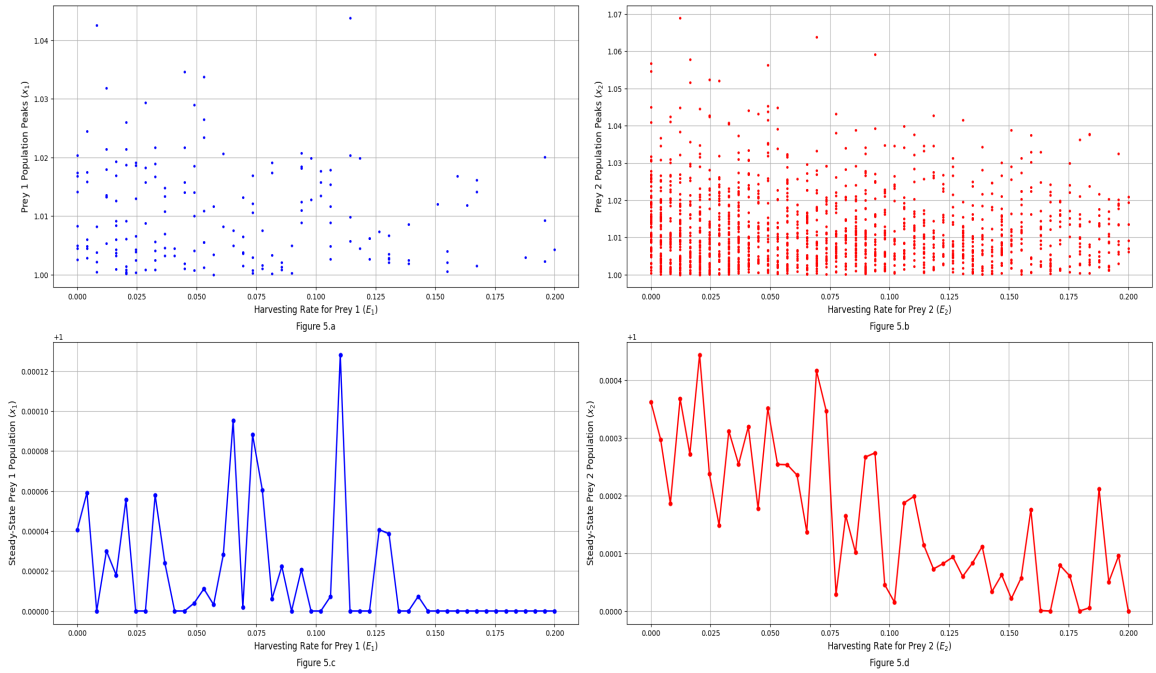

Figure 5: (a) Bifurcation diagram: local maxima of x_1 vs. E_1. (b) Bifurcation diagram: local maxima of x_2 vs. E_2. (c) Equilibrium of x_1 vs. E_1. (d) Equilibrium of x_2 vs. E_2. All plots are generated using parameters from Table 1.

Finally, the impact of harvesting intensity on prey dynamics is presented in Figure 5. Subfigures Figure 5 (a) and Figure 5 (b) display bifurcation diagrams showing the local maxima of sardine (x_1) and anchovy (x_2) populations as functions of their respective harvesting rates E_1 and E_2. Single peaks indicate stable equilibrium states, whereas multiple peaks signal oscillatory or chaotic regimes.

Subfigures Figure 5 (c) and Figure 5 (d) depict the corresponding equilibrium population levels, which exhibit monotonic decline as harvesting increases. These results demonstrate that while low harvesting promotes stability and sustainable yield, excessive harvesting destabilizes prey populations and drives them toward extinction. The findings emphasize the need for ecologically informed harvesting policies to maintain species persistence and system resilience.

8 Conclusion

This work presents a detailed examination of a stochastic predator-prey model for two small-forage fish prey species, sardines (*Sardinops sagax*) and anchovies (*Engraulis mordax*), and a predator blacktip shark (*Carcharhinus limbatus*) in the California Current Ecosystem (CCE). The model integrates Holling type-II

functional responses, prey fish harvesting, and stochastic perturbation to prey growth rates and predator mortality rates to reflect real-world complexity of ecological interactions and stochastic perturbations that dominate marine ecosystems. Theoretical analysis set forth a number of important results. First, the stochastic stability of the positive equilibrium was shown in the mean-square sense to prove that the system is still robust to small environmental fluctuations subject to certain parametric conditions (Theorem 3.2). This stability means that the expected squared departures of population densities from their equilibrium values are bounded, guaranteeing that small stochastic disturbances cannot cause the system to go to extinction. Existence and uniqueness of a global positive solution were also confirmed (Theorem 4.2), ensuring that the model generates biologically plausible results with non-negative population densities for all time, an essential prerequisite for ecological validity. In addition, stochastic persistence in the mean was established by deriving noise intensity thresholds under which populations can persist despite environmental variability (Section 5). Statistically, this implies that time-averaged population densities remain positive with probability one, indicating long-term survival. Furthermore, the existence of a stationary distribution under certain parameter regimes was proven in Section 6, providing insight into the long-term probabilistic dynamics of the system. This stationary distribution implies that, in the long term, the population densities settle to a stable probability distribution, allowing for the prediction of species abundance probabilities under environmental noise. These calculations emphasize the paramount importance of noise and harvesting in determining predator-prey behavior. The conditions of stability thus obtained, like the ones concerning the intensities α_1, α_2, and α_3 of noise, indicate the points beyond which random effects can trigger large-scale departures from equilibrium, even to the point of population extinction. For example, the predator's responsiveness to noise in its mortality rate, regulated by α_3, indicates that high environmental variability can disproportionately impact higher trophic levels, which agrees with ecological theory concerning trophic cascades. Also, the harvesting rates E_1 and E_2 on sardines and anchovies, respectively, determine the equilibrium of the system, where high harvesting causes a deviation from the balance, lowering prey and affecting predator survival. Statistically, this may be understood using the framework of bifurcation theory: with rising harvesting levels, the system can shift from a stable equilibrium to oscillatory or chaotic regimes, raising the variance in population densities and the probability of extinction events. The study highlights the need for careful control of environmental noise and rates of exploitation to maintain ecosystem stability, especially in the CCE, where sardine and anchovy fisheries are economically important and blacktip sharks are ecologically important. Sustainable harvesting practices, guided by the stability conditions derived, are necessary to avoid predator extinction and guarantee long-term coexistence of all species. For instance, keeping the rates of harvesting at subcritical levels maintains the population mean densities required for predator feeding, and managing environmental conditions (e.g., variation in temperature impacting α_1 and α_2) can buffer variance in prey growth rates. Additionally, adding stochasticity to ecological models is greatly beneficial for realistic projections, since deterministic models cannot fully model the range of effects of the environment on population processes. Statistically, this stochastic method enables the estimation of confidence intervals around population

trajectories, giving a probabilistic basis for evaluating extinction risks and guiding conservation policy. Further studies could also build upon this model by introducing further stochastic variables, including variance in rates of predation or climatic-modulated half-saturation constant alterations, to render it more realistic. Delving into spatially explicit models or systems of multi-predation could reveal deeper aspects into the CCE's greater ecological dynamics that aid more successful ecosystem-based fishery management. This study thus sets a strong framework for comprehending and managing marine ecosystems under the twin stresses of environmental stochasticity and human exploitation, emphasizing the fine balance necessary to preserve biodiversity and ecological stability.

References

[1] Kaplan, I. C., Koehn, L. E., Hodgson, E. E., Marshall, K. N., & Essington, T. E. (2017). Modeling food web effects of low sardine and anchovy abundance in the California Current. *Ecological Modelling, 359*, 1–24. https://doi.org/10.1016/j.ecolmodel.2017.05.007

[2] Kaplan, I. C., Francis, T. B., Punt, A. E., Koehn, L. E., Curchitser, E., Hurtado-Ferro, F., Johnson, K. F., Lluch-Cota, S. E., Sydeman, W. J., & Essington, T. E. (2019). A multi-model approach to understanding the role of Pacific sardine in the California Current food web. *Marine Ecology Progress Series, 617*, 307–321. https://doi.org/10.3354/meps12504

[3] Uriarte, A., Alday, A., Santos, M., & Motos, L. (2012). A re-evaluation of the spawning fraction estimation procedures for Bay of Biscay anchovy, a species with short interspawning intervals. *Fisheries Research, 117*, 96–111. https://doi.org/10.1016/j.fishres.2011.03.002

[4] Mantua, N. J., Hare, S. R., Zhang, Y., Wallace, J. M., & Francis, R. C. (1997). A Pacific interdecadal climate oscillation with impacts on salmon production. *Bulletin of the American Meteorological Society, 78*(6), 1069–1080. https://doi.org/10.1175/1520-0477(1997)078<1069:APICOW>2.0.CO;2

[5] Checkley, D. M. Jr., Asch, R. G., & Rykaczewski, R. R. (2017). Climate, anchovy, and sardine. *Annual Review of Marine Science, 9*(1), 469–493. https://doi.org/10.1146/annurev-marine-122414-033819

[6] Mao, X. (2007). *Stochastic differential equations and applications*. Elsevier. https://doi.org/10.1007/978-3-642-11079-5_2

[7] Buffoni, G., Groppi, M., & Soresina, C. (2016). Dynamics of predator–prey models with a strong Allee effect on the prey and predator-dependent trophic functions. *Nonlinear Analysis: Real World Applications, 30*, 143–169. https://doi.org/10.1016/j.nonrwa.2015.12.001

[8] Mahapatra, G. S., & Santra, P. (2016). Prey–predator model for optimal harvesting with functional response incorporating prey refuge. *International Journal of Biomathematics, 9*(1), 1650014. https://doi.org/10.1142/S1793524516500145

[9] Das, K. P., Chatterjee, S., & Chattopadhyay, J. (2010). Occurrence of chaos and its possible control in a predator-prey model with density dependent disease-induced mortality on predator population. *Journal of Biological Systems, 18*(2), 399–435. https://doi.org/10.1142/S0218339010003391

[10] Banerjee, C., Das, P., & Roy, A. B. (2015). Stability, bifurcations and chaotic dynamics in a delayed hybrid tri-trophic food chain model with Holling type-II and Leslie-Gower type functional responses. *World Journal of Modelling and Simulation, 11*(3), 174–198. https://www.researchgate.net/publication/283778884_Stability_bifurcations_and_chaotic_dynamics_in_a_delayed_hybrid_tri-trophic_food_chain_model_with_Holling_type-II_and_Leslie-Gower_type_functional_responses

[11] May, R. M. (2019). *Stability and complexity in model ecosystems*. Princeton University Press. https://doi.org/10.2307/j.ctvs32rq4

[12] Liu, Q., Zu, L., & Jiang, D. (2016). Dynamics of stochastic predator–prey models with Holling II functional response. *Communications in Nonlinear Science and Numerical Simulation, 37*, 62–76. https://doi.org/10.1016/j.cnsns.2016.01.005

[13] Zuo, W., & Jiang, D. (2016). Stationary distribution and periodic solution for stochastic predator-prey systems with nonlinear predator harvesting. *Communications in Nonlinear Science and Numerical Simulation, 36*, 65–80. https://doi.org/10.1016/j.cnsns.2015.11.014

[14] Jana, D., Agrawal, R., & Upadhyay, R. K. (2015). Dynamics of generalist predator in a stochastic environment: Effect of delayed growth and prey refuge. *Applied Mathematics and Computation, 268*, 1072–1094. https://doi.org/10.1016/j.amc.2015.06.098

[15] Aguirre, P., González-Olivares, E., & Torres, S. (2013). Stochastic predator–prey model with Allee effect on prey. *Nonlinear Analysis: Real World Applications, 14*(1), 768–779. https://doi.org/10.1016/j.nonrwa.2012.07.032

[16] Lv, J., & Wang, K. (2011). Asymptotic properties of a stochastic predator–prey system with Holling II functional response. *Communications in Nonlinear Science and Numerical Simulation, 16*(10), 4037–4048. https://doi.org/10.1016/j.cnsns.2011.01.015

[17] Liu, Z., Shi, N., Jiang, D., & Ji, C. (2012). The asymptotic behavior of a stochastic predator-prey system with Holling II functional response. *Abstract and Applied Analysis, 2012*(1), 801812. https://doi.org/10.1155/2012/801812

[18] Mandal, P. S., & Banerjee, M. (2012). Stochastic persistence and stationary distribution in a Holling–Tanner type prey–predator model. *Physica A: Statistical Mechanics and its Applications, 391*(4), 1216–1233. https://doi.org/10.1016/j.physa.2011.10.019

[19] Gard, T. C. (2000). Transient effects of stochastic multi-population models. *Preprint*. https://www.researchgate.net/publication/26393530_Transient_effects_of_stochastic_multi-population_models

[20] Allen, E. (2007). *Modeling with Itô stochastic differential equations*. Springer. https://link.springer.com/book/10.1007/978-1-4020-5953-7

[21] Wilkinson, D. J. (2018). *Stochastic modelling for systems biology.* Chapman & Hall/CRC. https://doi.org/10.1201/9781351000918

[22] Gani, J., & Swift, R. J. (2008). An unexpected result in an approximate carrier-borne epidemic process. *Statistics & Probability Letters, 78*(14), 2116–2120. https://doi.org/10.1016/j.spl.2008.01.077

[23] Baishya, M. C., & Chakraborti, C. G. (1987). Non-equilibrium fluctuation in Volterra-Lotka systems. *Bulletin of Mathematical Biology, 49*, 125–131. https://doi.org/10.1007/BF02459962

[24] Bandyopadhyay, M., & Chakrabarti, C. G. (2003). Deterministic and stochastic analysis of a nonlinear prey-predator system. *Journal of Biological Systems, 11*(2), 161–172. https://doi.org/10.1142/S0218339003000816

[25] Carletti, M. (2002). On the stability properties of a stochastic model for phage–bacteria interaction in open marine environment. *Mathematical Biosciences, 175*(2), 117–131. https://doi.org/10.1016/S0025-5564(01)00089-X

[26] Allen, L. J. S. (2010). *An introduction to stochastic processes with applications to biology.* CRC Press. https://doi.org/10.1201/b12537

[27] Lindegren, M., Checkley, D. M. Jr., Rouyer, T., MacCall, A. D., & Stenseth, N. C. (2013). Climate, fishing, and fluctuations of sardine and anchovy in the California Current. *Proceedings of the National Academy of Sciences, 110*(33), 13672–13677. https://doi.org/10.1073/pnas.1305733110

[28] Turelli, M. (1977). Random environments and stochastic calculus. *Theoretical Population Biology, 12*(2), 140–178. https://doi.org/10.1016/0040-5809(77)90040-5

[29] May, R. M. (1976). Simple mathematical models with very complicated dynamics. *Nature, 261*(5560), 459–467. https://www.nature.com/articles/261459a0

[30] Clark, C. W. (2010). *Mathematical bioeconomics: The mathematics of conservation.* John Wiley & Sons.

[31] Tuck, G. N., & Possingham, H. P. (2003). Bioeconomy – Economically optimal spatial and inter-temporal fishing patterns in a metapopulation. In *Marine protected areas: A multidisciplinary approach* (Chapter 4). Cambridge University Press. https://doi.org/10.1017/CBO9781139049382.007

[32] Braumann, C. A. (2002). Variable effort harvesting models in random environments: Generalization to density-dependent noise intensities. *Mathematical Biosciences, 177*, 229–245. https://doi.org/10.1016/S0025-5564(01)00110-9

[33] Ma, Y., & Yu, X. (2024). Stochastic analysis of survival and sensitivity in a competition model influenced by toxins under a fluctuating environment. *AIMS Mathematics, 9*(4), 8230–8249. https://doi.org/10.3934/math.2024400

[34] Sha, A., Roy, S., Tiwari, P. K., & Chattopadhyay, J. (2024). Dynamics of a generalist predator–prey system with harvesting and hunting cooperation in deterministic/stochastic environment. *Mathematical Methods in the Applied Sciences, 47*(7), 5916–5938. https://doi.org/10.1002/mma.9897

[35] Reis, M., Brites, N. M., Santos, C., & Dias, C. (2024). Comparison of optimal harvesting policies with general logistic growth and a general harvesting function. *Mathematical Methods in the Applied Sciences, 47*(10), 8076–8088. https://doi.org/10.1002/mma.10004

[36] Edwards, H., & Penney, D. (1999). *Differential equations and boundary value problems* (2nd ed.). Prentice Hall.

[37] Kolmanovskii, V. B., & Shaikhet, L. E. (2002). Some peculiarities of the general method of Lyapunov functionals construction. *Applied Mathematics Letters, 15*, 355–360. https://doi.org/10.1016/S0893-9659(01)00143-4

[38] Kolmanovskii, V. B., & Shaikhet, L. E. (2002). Construction of Lyapunov functionals for stochastic hereditary systems: A survey of some recent results. *Mathematical and Computer Modelling, 36*, 691–716. https://doi.org/10.1016/S0895-7177(02)00168-1

[39] Birkhoff, G., & Rota, G. C. (1982). *Ordinary differential equations*. Ginn.

[40] Hasminskii, R. Z. (1980). *Stochastic stability in differential equations*. Sijthoff and Noordhoff. https://doi.org/10.1007/978-94-009-9121-7

[41] Arnold, L. (1972). *Stochastic differential equations: Theory and applications*. Wiley.

[42] Friedman, A. (1976). *Stochastic differential equations and their applications*. Academic Press.

[43] Gard, T. C. (1987). *Introduction to stochastic differential equations*. Marcel Dekker.

[44] Mao, X. (1997). *Stochastic differential equations and applications*. Horwood.

[45] Liu, M., Wang, K., & Wu, Q. (2010). Survival analysis of stochastic competitive models in a polluted environment and stochastic competitive exclusion principle. *Bulletin of Mathematical Biology*. https://doi.org/10.1007/s11538-010-9569-5

[46] Allen, L. J. S. (2003). *An introduction to stochastic processes with applications to biology*. Pearson Education.

[47] Ackleh, A. S., Allen, L. J. S., & Carter, J. (2007). Establishing a beachhead: A stochastic population model with an Allee effect applied to species invasion. *Theoretical Population Biology, 71*(3), 290–300. https://doi.org/10.1016/j.tpb.2006.12.006